rather inert with respect to chemical surface reactions. It has been shown that nonreactive interfaces between layered semiconductors and metals show Schottky limit behavior, whereas reactive interfaces show Fermi-level pinning.[24,25] Many metal adsorbates tend to cluster on the van der Waals (0001) plane of layered semiconductors (Volmer-Weber growth)[25-32] making such metal/semiconductor interfaces ideal model systems for investigating laterally inhomogeneous Schottky barriers.

In this paper we present investigations of the *p*-$WSe_2$/In interface. The interaction of deposited In with layered semiconductors has been previously studied.[33-36] The interfaces have been found to be nonreactive and with barrier heights close to the Schottky limit. As already published elsewhere[36] In deposited onto $WSe_2$ (0001) faces has a strong tendency to form three-dimensional islands (metal clusters) at room temperature.

In this investigation the $WSe_2$/In interface was systematically studied under different conditions with photoelectron spectroscopy [ultraviolet photoemission spectroscopy (UPS), (soft) x-ray photoemission spectroscopy (S) XPS], scanning electron microscopy (SEM), scanning tunneling microscopy (STM), and electron microprobe. In the first set of experiments the formation of the interface was investigated at room temperature (300 K). At this temperature a strong tendency for cluster growth is observed (Volmer-Weber growth). In the following experiments indium was deposited at low substrate temperature (LT), where the In layer shows layer by layer growth (Frank-van der Merwe growth). Upon warming to room temperature a morphology change to the clustered state occurs. This change in metal overlayer morphology makes the In/$WSe_2$ system ideal for comparing electronic properties at laterally homogeneous and inhomogeneous interfaces.

## II. EXPERIMENT

Most of the room-temperature (RT) deposition experiments were performed in a VG ESCALAB Mk II system with an additional evaporation chamber. The base pressure of the system was $5\times10^{-11}$ mbar. For all XPS experiments we used Mg $K\alpha$ radiation. The UPS measurements were performed with He I and He II light. For the LT deposition experiments we used a VG ADES 500 system with a base pressure of $1\times10^{-10}$ mbar. The photoemission experiments were performed with synchrotron radiation (BESSY storage ring, TGM7-beam line, $h\nu=66$ eV). All presented core-level line positions and full widths at half maximum (FWHM's) are obtained by curve fitting using a function proposed by Kojima and Kurahashi.[37] The spectra were referred to the Fermi edge of the sputtered copper sample holder and are given in binding energies (BE's). The work functions $\Phi$ were determined from the secondary-electron onset (negative bias applied to the sample).

Single crystals of *p*-type $WSe_2$ were prepared by chemical-vapor transport (CVT) in sealed quartz tubes. Se was used as the transport agent. Hall measurements on all crystals showed a doping density in the range of $10^{17}$ $cm^{-3}$. Typical areas of the crystals were $5\times5$ $mm^2$.

The specimens were attached to the Cu sample holders by Ag epoxy and cleaved in UHV. Perfectly clean and mirrorlike surfaces were obtained by this procedure. Low-energy electron diffraction (LEED) measurements show bright and sharp hexagonal patterns as expected for the (0001) surfaces. No band bending at the surface was observed after cleaving as the valence-band onset was measured close to the Fermi energy in agreement with the Hall-effect measurements. In addition, no surface photovoltage shifts by additional bias illumination (Tungsten halogen lamp, $\approx100$mW $cm^{-2}$) could be observed, as expected for flat-band conditions at the surface. We also did not observe any BE shifts of the cleaved substrate by cooling in the dark and with bias illumination, which excludes charging effects of the sample and the back contact.

The sample temperature was measured with a thermocouple attached to the manipulator near the sampleholder. A quartz microbalance was used for evaporation rate control of the In source which was calibrated before every evaporation step. All given coverages are an average over the whole surface and do not correspond to actual overlayer thicknesses at a particular site.

SEM and STM measurements were performed *ex situ*. For the SEM measurements a Cambridge Instruments S253 system was used at 20-kV acceleration voltage. The STM pictures were measured with a Nanoscope II system.

## III. RESULTS

### A. Deposition at 300-K substrate temperature

#### 1. *Interface formation*

Indium was evaporated in small increments from submonolayer coverages to 560-Å-thick layers. The UPS and XPS data obtained after each deposition step are presented in Figs. 1 and 2, respectively. For the cleaved *p*-$WSe_2$ (0001) surface valence-band and core-level spectra agree with previously published data.[38] The core lines do not show any changes due to chemical shifts with deposition of indium (Fig. 2). In addition the W/Se intensity ratio does not change with In coverage (Fig. 3). The valence-band spectra show up as a superposition of emission intensity from the $WSe_2$ substrate and from the In overlayer (Fig. 1). From this we conclude that the interface is atomically abrupt and nonreactive in agreement with previously published results on In deposition on layered semiconductors.[33-35] We only observe a shift of the substrate emissions due to band bending.

With increasing In coverage strong core-level emission lines grow in at a constant binding energy (BE is 16.8 eV) typical for metallic indium. A Fermi edge of the metallic In overlayer is clearly developed in the He I and He II spectra only for coverages larger than 80 Å. Its position is equivalent to the reference Fermi level excluding shifts due to SPV effects (compare He I spectra, Fig. 1).

The secondary-electron onset of the indium-covered surface shows two contributions: one at higher BE, which is related to the semiconductor substrate ($\Phi=5.2\pm0.1$

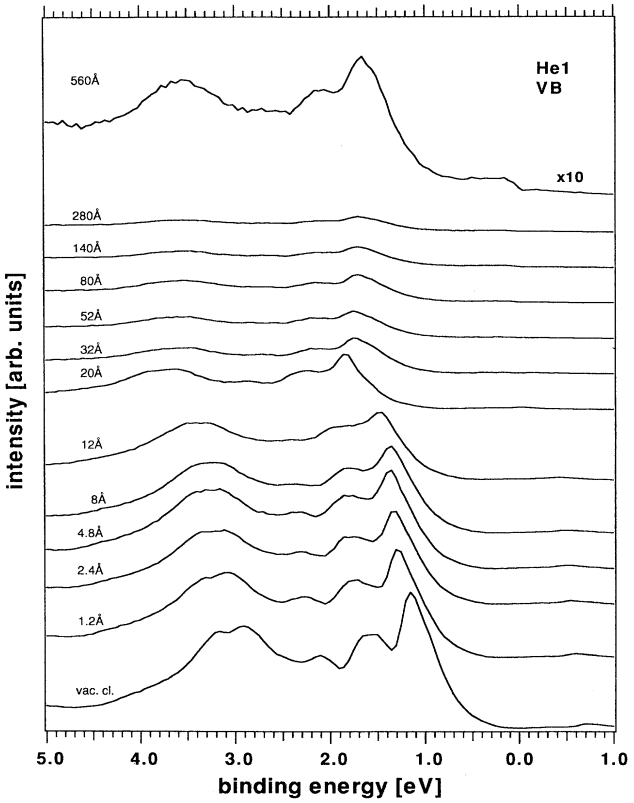


FIG. 1. He I valence-band spectra of the $WSe_2$ (0001)/In interface with increasing nominal In coverage at 300 K.

eV for uncovered surface) and one at lower BE, which is attributed to the In clusters ($\Phi = 4.1 \pm 0.1$ eV). In spite of the strong increase of In emission lines the substrate core line intensities are only weakly attenuated. Even at the final In coverage of 560 Å the W 4*f* emissions can still be measured. Compared to the mean free path of photoelectrons at this energy (approximately 40 Å) it indicates a three-dimensional cluster growth of the In overlayer

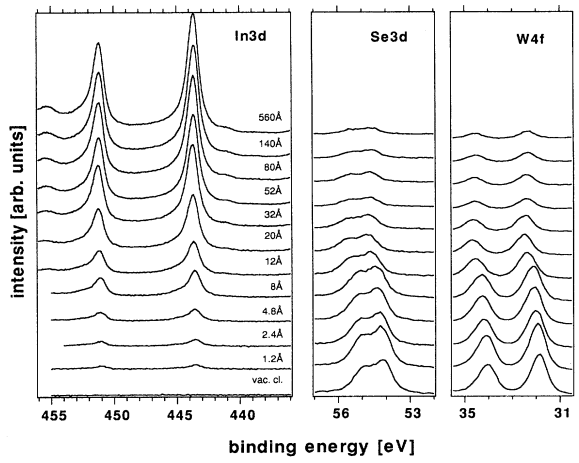


FIG. 2. Mg $K\alpha$ core-level spectra of the $WSe_2$ (0001)/In interface with increasing nominal In coverage at 300 K.

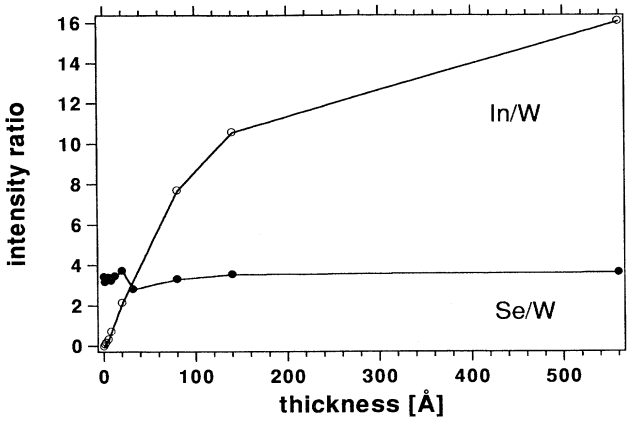


FIG. 3. Plot of the In/W and Se/W XPS intensity ratios (corrected by theoretical cross sections) as a function of nominal In coverage (taken from Fig. 2).

(Volmer-Weber growth mode). Even in the more surface sensitive UP valence-band spectra (Fig. 1) we are still able to identify substrate emission up to the nominal coverage of 560 Å. In Fig. 3 we show the In/W intensity ratio. The shape of the curve is characteristic for Volmer-Weber growth.[39] In order to complement the photoemission data on the In cluster growth we performed *ex situ* electron microscopy studies of the In interface. In Fig. 4 SEM pictures of two samples [with 80 Å (a) and 560 Å (b) coverage] are shown. Both pictures show distinguished areas of indium covered (bright) and uncovered (dark) parts of the surface. We were not able to detect any indium between the bright areas with microprobe measurements. The size and the lateral separation of the clusters can be estimated from the SEM pictures. For both coverages a broad distribution of cluster sizes is obtained. The clusters are separated from each other by approximately 0.5–1 $\mu$m but also with a wide distribution of smaller and larger distances.

The actual cluster height was determined by STM. A $WSe_2$ sample was covered with a 40-Å In layer. Figure 5 shows a $3 \times 3$ $\mu m^2$ area of this sample with In elevations of approximately 120 Å height and 5000 Å lateral extension. The STM pictures also show an average intercluster distance around 0.5–1 $\mu$m. Most clusters are aligned in triangular shapes indicating epitaxial growth of the metal overlayer on the hexagonal substrate. However, this was not confirmed by LEED. At increasing coverage the LEED spots transform into a diffuse background. Evidently we do not have a definite long-range order of the deposited In overlayer as has been found for Cu, Ag, and Au deposition.[25,31] It should be noted that it was very difficult to obtain sharp STM pictures. Most scanned areas did not stand a second scan indicating very weak interactions between the adsorbate and substrate. In summary, indium deposited onto $WSe_2$ (0001) surfaces at room temperature forms three-dimensional metallic clusters which are separated from each other by bare areas of the substrate.

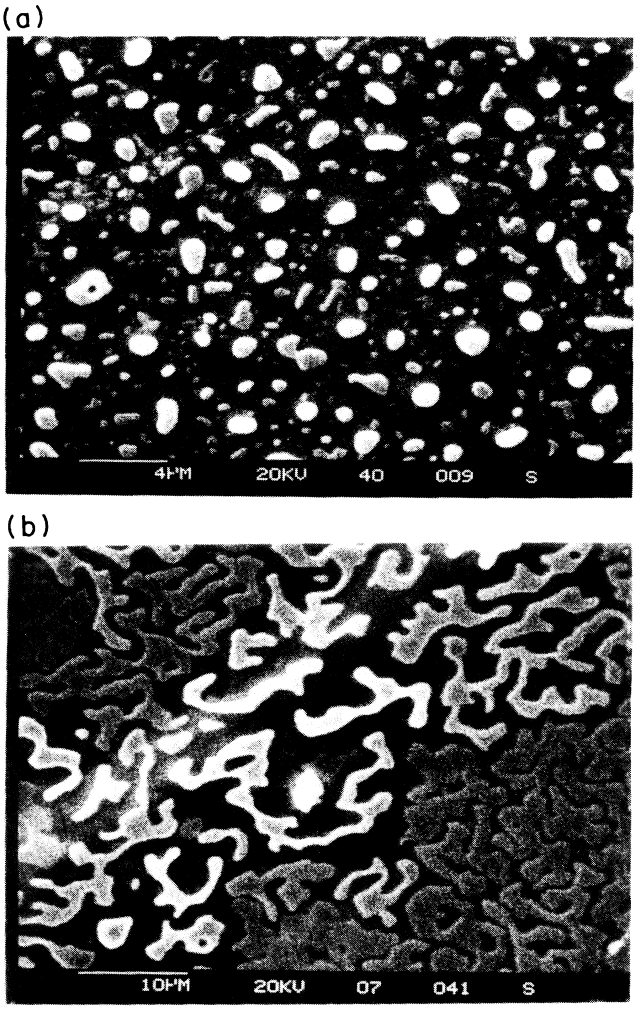


FIG. 4. Scanning-electron-microscope pictures of the $WSe_2$/In interface for different nominal coverages [(a) 80 Å, (b) 560 Å].

*2. Band bending and surface-photovoltage measurements*

The band bending $eV_b$ as a function of coverage, determined from the shifts of W $4f$ (XPS) and W $5d_{z^2}$ (UPS) emissions, is shown in Fig. 6. At 20-Å coverage we observe a maximum value of 0.7 eV. At higher coverages $eV_b$ decreases again to a final value of 0.55 eV. The development of $eV_b$ is tentatively related either to a change of cluster (adatom) distribution from smaller to higher doses, and/or to a change of the work function of the In clusters during growth. The measured barrier height is too low when compared to the theoretically predicted value. Based on the work function difference between indium ($\Phi = 4.1$ eV) and $p$-$WSe_2$ ($\Phi = 5.2$ eV) a band bending of 1.1 eV should have been obtained according to the Schottky limit. A rebending due to x-ray or uv induced SPV can be excluded from either the position of the In core levels or from the Fermi-level position which were unshifted at 300 K.

The saturation value of $eV_b$ is established considerably slower than usually measured for Schottky barriers formed on the more intensively studied III-V compounds, where the final Fermi-level position is often reached for submonolayer coverage. We attribute this fact to the tendency of cluster formation on the layered substrate as similar curves were found for other nonreactive layered semiconductor/metal combinations as $WSe_2$/Au and $MoS_2$/Au.[25,40]

To gain more insight into the junction properties the SPV induced by additional bias illumination (W halogen lamp, $\approx 100$ mW/cm$^2$) was investigated.

After every evaporation step we measured the spectra with and without bias light, both at room temperature and at 150 K. In Fig. 7 we show the UPS binding energy positions of the substrate W $5d_{z^2}$ line (a) and the adsorbate In $4d$ line (b) as a function of the nominal In coverage. The figures show the binding energy positions at 300 K (circles) and 150 K (squares) measured in darkness (filled markers) and with bias illumination (unfilled mark-

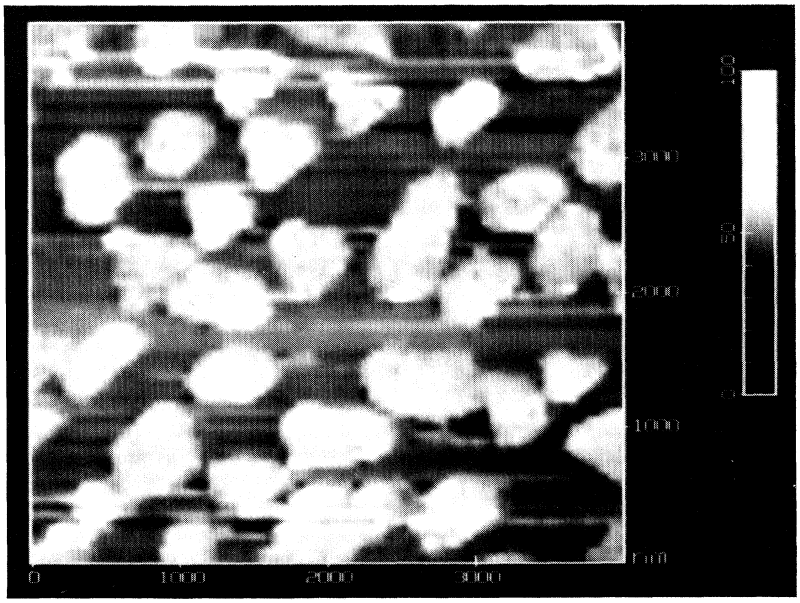

FIG. 5. Scanning-tunneling-microscope picture of the $WSe_2$/In interface at a nominal coverage of 40 Å.

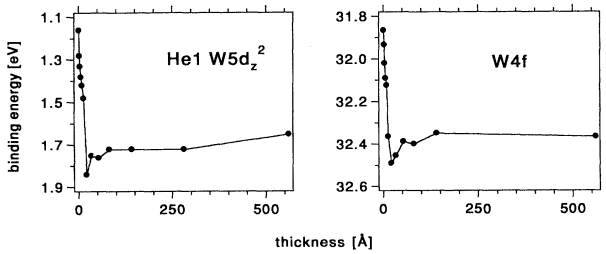


FIG. 6. Binding energy shifts due to band bending at the $WSe_2$ (0001)/In interface as function of nominal In coverage (taken from Figs. 1 and 2).

ers). At 300 K both emission lines show only very weak SPV shifts in the range of 0.1 V. When cooled down the SPV shifts are increased up to 0.6 V. Moreover a SPV is already present without bias illumination caused by the photoemission source itself. Comparing the two graphs, it is obvious that the In 4*d* shifts are larger than the W $5d_{z^2}$ shifts. The SPV values do not depend on the photoemission excitation source. In Fig. 8 we show these photovoltage differences at 150 K with additional bias illumination as a function of coverage. The graphs are obtained by subtracting the 300-K dark binding energies from the 150-K illuminated line positions. The SPV difference is larger for small coverages. The maximum In 4*d* SPV (0.6 V) exceeds even the band bending as determined from the substrate emissions (0.5 eV). This indicates that the band bending below the In clusters must be larger than the band bending measured from the substrate BE shifts. It should be noted that even at lower coverages the thickness of the In clusters is large compared to the escape depth of the photoelectrons so that the substrate emission originates only from bare areas between clusters.

### B. Deposition at 100-K substrate temperature

#### 1. Morphology of the interface

Evidence for inhomogeneous band bending should be obtained by determining the band bending directly below the In clusters or below an unclustered interface. Therefore, we deposited In in small steps onto a sample kept at a temperature of about 100 K. We obtained a homogeneous In overlayer. In Fig. 9 valence-band spectra and in Fig. 10 W 4*f* and In 4*d* core-level spectra of this $WSe_2$/In interface are presented for different experimental conditions. All spectra were taken without additional bias illumination. It is interesting to mention the occurrence of "wiggles" in the valence-band spectrum for 1 Å coverage. We tentatively assign these wiggles to quantum-size effects (QSE) in small In clusters as observed for Ag deposited on GaAs(110) by Evans *et al.*[41] As QSE are beyond the scope of this paper we will report on these effects elsewhere. Compared to the RT deposition results the substrate emissions are diminishing faster and the In emissions grow in more rapidly. After 20-Å nominal In coverage no substrate valence band or core-level features can be detected anymore. For the measured electron kinetic energies the electron mean free path is less than 10 Å. Hence it follows that indium grows at this temperature layer by layer (Frank–van der Merwe growth mode) forming a laminar In overlayer. In addition, the Fermi edge of the In overlayer is already developed after 5-Å nominal In thickness.

While warming up to 300 K the spectra show dramatic changes in shape which we relate to clustering of the indium overlayer. Beginning very slowly at about 150 K this transformation accelerates in the temperature range near 200 K. The main feature of this transformation is the increase of $WSe_2$ emissions in the range between 0 and 3 eV binding energy and the decrease of the Fermi edge. This process is almost finished in the spectrum taken at 201 K.

Additional evidence for the In overlayer morphology change is given by the intensity of substrate and In overlayer core-level spectra (Fig. 10). During warm up to 300 K the substrate intensity increases accompanied by a decrease of In emissions. From a plot of the W 4*f* and In 4*d* intensities versus temperature (Fig. 11) the transition point of the In overlayer transformation can be determined to occur between 160 and 200 K. The In emission peaks at about 235 K show an interesting structure characterized by a broad feature without the expected multiplet splitting which is reestablished at 300 K. This is related to inhomogeneous electric potential distributions occurring during the morphology transition as will be discussed in detail in the next chapter. Line broadening and asymmetric line shapes were also observed for the W 4*f* core levels in the same temperature range.

#### 2. Band bending and SPV

In Fig. 12 the BE shifts of the W 4*f* and In 4*d* emission lines are summarized in relation to the BE measured on

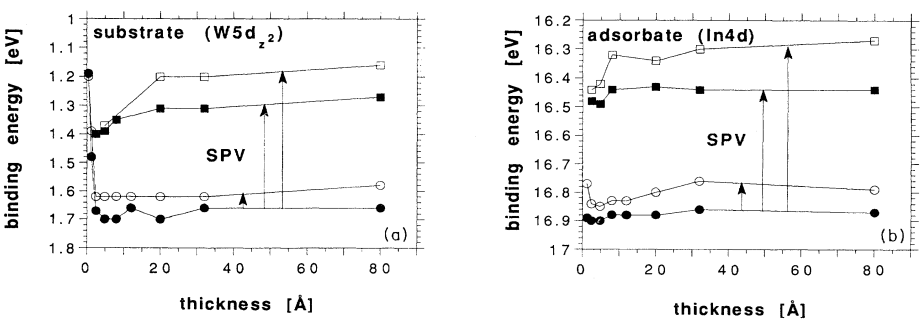


FIG. 7. Binding energy shifts of the $WSe_2$ (0001)/In interface due to band bending and SPV as function of nominal In coverage for different conditions: (a) substrate BE shifts, (b) adsorbate BE shifts [black circles: room temperature (RT); no bias light; white circles: RT, bias light; black rectangles: 150 K, no bias light; white rectangles: 150 K, bias light].

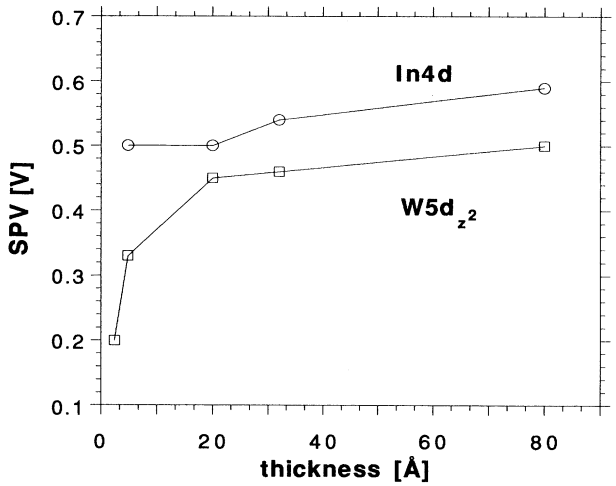


FIG. 8. Comparison of SPV shifts of substrate and overlayer as given in Fig. 7 (difference of the RT–no bias light curve to the 150 K–bias light curve).

cleaved $WSe_2$ and on metallic In on the Cu sample holder (BE is 16.8 eV), respectively. The source-induced SPV of the indium-covered areas of the surface was deduced from Fermi edge and In 4*d* line shifts (Figs. 9 and 10). The band-bending value obtained after SPV correction of the measured W 4*f* shifts are also shown in Fig. 12.

The W 4*f* spectrum taken after 10-Å indium coverage shows a measured band bending of about 0.6 eV. Corrected for SPV (0.4 V) an equilibrium band bending of about 1 eV is determined below the In overlayer. At 20-Å coverage the W 4*f* emission disappears, but appears again at about 188 K during warming up. At this moment the measured band bending amounts to 0.85 eV with a SPV $<0.1$ V. This maximum uncorrected W 4*f* BE shift provides a minimum value for the actual band bending below the In metal layers which is at least 0.3 eV larger than the band bending determined from substrate core-level shifts of the RT experiment (Fig. 6). However,

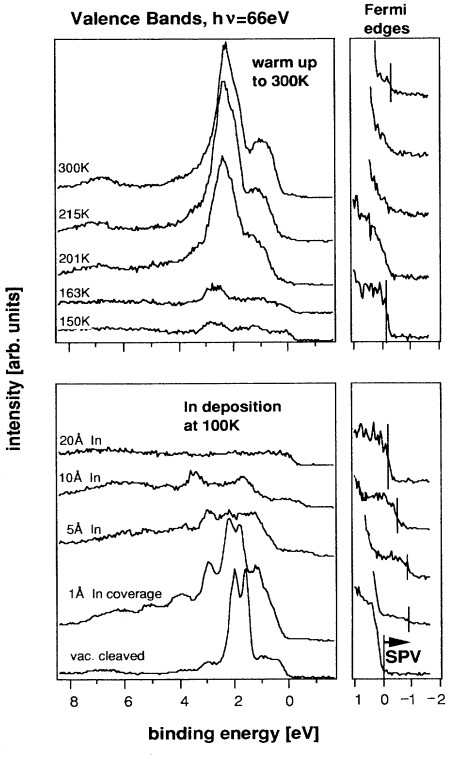


FIG. 9. SXP valence-band spectra ($h\nu=66$ eV) of the $WSe_2$/In interface with increasing nominal coverage at 100 K (lower part) and during warm-up to 300 K (the Fermi-edge region is shown enlarged on the right).

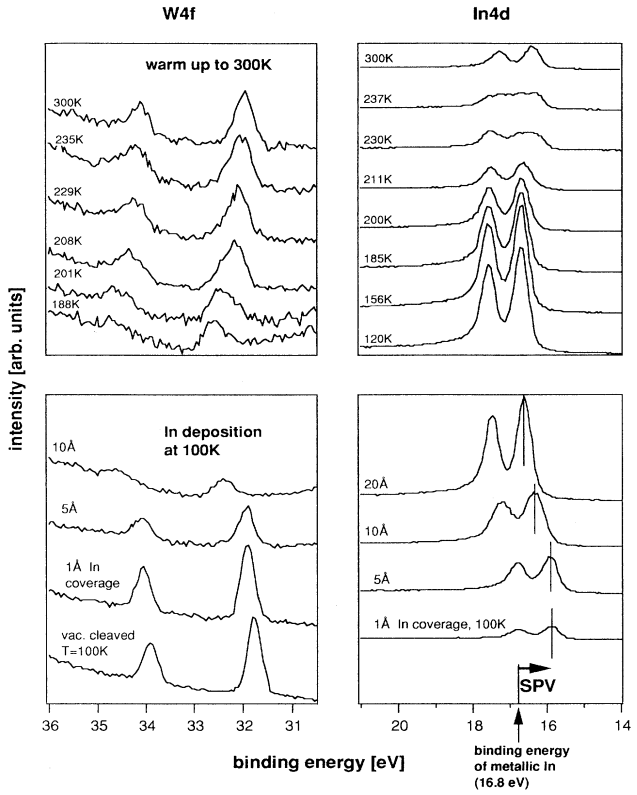


FIG. 10. SXP core-level spectra ($h\nu=66$ eV) of the $WSe_2$/In interface with increasing nominal coverage at 100 K (lower part) and during warm-up to 300 K.

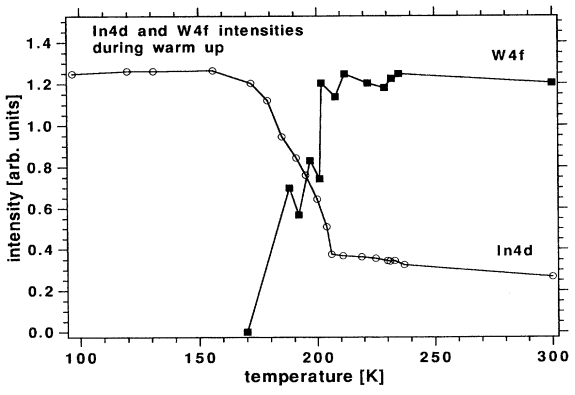


FIG. 11. Plot of the In and W SXPS intensities as a function of sample temperature during warm-up (compare Fig. 10).

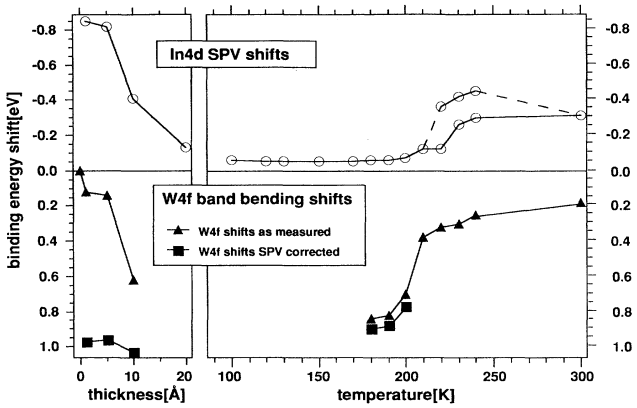


FIG. 12. Binding energy shifts due to band bending and SPV at the $WSe_2$/In interface for different experimental conditions.

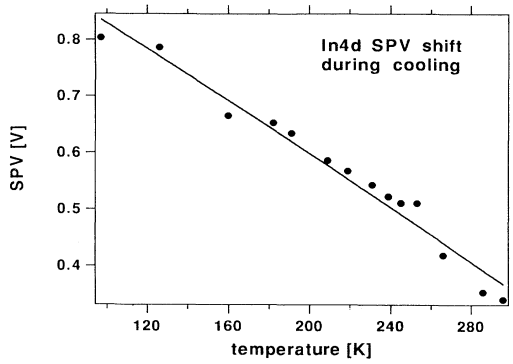


FIG. 14. In 4*d* binding energy shifts due to SPV during recooling of the reclustered $WSe_2$ (0001)/In interface. The drawn line represents the result of a least-squares fit (see text for details).

at 300 K, after the morphology change of the interface has been completed, the measured W 4*f* BE shift is only 0.2 eV (Fig. 12). The difference to the saturation value in the RT experiment (Fig. 6) is attributed to the smaller In coverage which results in larger uncovered areas between the In clusters. In addition, there may be a small SPV shift. However, it should be considerably smaller than the SPV measured for In covered areas (0.3 V).

Also the SPV is strongly affected by the morphology of the interface. Compared to the BE value of metallic In on Cu (BE is 16.8 eV) all In 4*d* spectra show SPV shifts. After 1 Å coverage the In 4*d* position is located at 15.85 eV. This amounts to a SPV of 0.85 V in agreement with the shift of the Fermi edge in the valence-band spectra (Fig. 9). During the following evaporation steps the SPV decreases to 0.1 V at 20 Å coverage. Thus, the SPV is drastically reduced as a function of increasing In coverage as often observed in Schottky barrier formation with laminar overlayers. The decrease in SPV is attributed to the leakage currents due to the increased surface conductivity of the metal overlayer.[22,42]

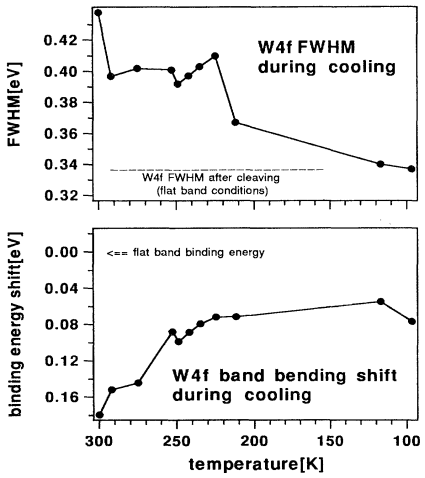


FIG. 13. Changes of W 4*f* FWHM and binding energy during recooling of the reclustered $WSe_2$ (0001)/In interface. The given flat-band FWHM reference value of 0.34 eV was measured at 100 K (RT is 0.35 eV).

It is obvious that the clustering (starting at a sample temperature of 150 K) is again accompanied by a SPV increase, although the diode reverse dark current rises with temperature and should result in a decrease of SPV. At 300 K the SPV of In-covered areas amounts to 0.3 V. In the In 4*d* spectra between 219 and 237 K (Fig. 10) the observed broadening is thus related to the coexistence of clustered and nonclustered areas which are electrically connected in a different way to defects or to the sample holder, giving rise to different shunt resistances.

### 3. *Temperature dependence of SPV at the clustered interface*

In order to obtain additional information on the energetic conditions of the clustered *p*-$WSe_2$/In interface the sample was recooled to 100 K after warming to 300 K and the SPV was determined as a function of temperature. During cooling the W 4*f* and In 4*d* spectra do not change their shape or intensity ratio indicating that the cluster morphology remains unchanged. Both emission lines show shifts due to increasing SPV (Figs. 13 and 14). The In 4*d* line shifts from 16.4 to 15.9 eV corresponding to an increase of SPV by 0.5 V. Thus, at 100 K the SPV again amounts to 0.8 V which reproduces the maximum observed SPV for the low In coverage at 100 K. In contrast the shift of the W 4*f* peaks, due to SPV, is only about 0.1 eV. The FWHM's of the W 4*f* line decreases during cooling from 0.44 to 0.34 eV (see Fig. 13) whereas the FWHM of the In 4*d* line remains the same (0.5 eV).

## IV. DISCUSSION

### A. Morphology of the interface

Corresponding with recently published results on GaAs/In (Refs. 17, 19, and 43–45) the system *p*-$WSe_2$/In also exhibits a pronounced sample temperature-dependent change in interface morphology. When evaporated at a sample temperature of 300 K indium films grow in the Volmer-Weber mode whereas at 100 K layer-by-layer growth is observed. (Clustering of the In

films occurs at annealing temperatures of 150–200 K.) The interface remains nonreactive and atomically abrupt for all experimental conditions. The observed instability of the clusters during STM measurements indicate very weak interaction between In clusters and $WSe_2$ surface. In many scanned areas the clusters were "wiped" away during measurement. Nevertheless we were able to determine their shape by STM and SEM measurements. The In clusters have a diameter of about 0.5–1 $\mu$m with gaps of the same magnitude. The height of the clusters is typically in the range of 100 Å which is considerably smaller than the lateral extension. Many clusters show pronounced aligned shapes with 60 ° angles suggesting epitaxial cluster growth. This *ex situ* determination of cluster shape and intercluster distance should be considered with some care. The original distribution and morphology of In clusters may be different because of the high surface mobility. In addition, the morphology is probably different at different stages of the experiment and for different runs. At RT deposition a more scattered distribution of smaller clusters with smaller intercluster distances will initially be formed which will coalesce to larger clusters with increased distances at higher coverages (compare calculations in Ref. 19). Furthermore, the size and number of clusters obtained from the LT deposition experiment is rather small. Therefore only a qualitative comparison of cluster morphology and related electronic properties is possible for the different experiments.

### B. Barrier inhomogeneities of the clustered interface

According to the Schottky limit the band bending $eV_b$ is given by the difference of the work functions of semiconductor and metal. Therefore the system $p$-$WSe_2$/In [$p$-$WSe_2$: $\Phi = 5.2 \pm 0.1$ eV, obtained from the secondary-electron onset of He I spectra after cleaving in vacuum; indium: $\Phi = 4.1$ eV (Ref. 46)] should result in a band bending of $1.1 \pm 0.1$ eV, which is nearly the maximum possible value for $WSe_2$ (band gap, 1.2 eV). However, in our 300-K experiment $eV_b$ is only 0.55 eV as determined from the substrate core-level shifts of the In free areas (no x-ray induced SPV). But, the bias light SPV shifts for the In 4$d$ overlayer emissions after cooling exceed $eV_b$ and the SPV shifts of the substrate W 4$f$ emission lines. Suggesting that the band bending at the interface is laterally inhomogeneous, the actual band bending below the In clusters must be larger than the measured value determined from BE shifts of substrate emissions coming from bare areas.

In Fig. 15 this laterally inhomogeneous potential distribution is schematically drawn. The spatial development of band bending near an In cluster is shown in the lower part of the picture (in this part the $z$ axis is rotated by 90 °). From this model it is obvious that the measured substrate line positions represent an average over the whole uncovered surface. The mean In cluster distance $d_{\mathrm{In}}$ can be estimated from the STM and SEM pictures. For low nominal In coverages (80 Å) $d_{\mathrm{In}}$ is about 5000 Å and for high In coverages (560 Å) $d_{\mathrm{In}}$ is about 1000 Å. These values must be compared to the lateral extension $d_s$ of the space charge layer. In the depletion approximation the expression for $d_s$ is given by[3]

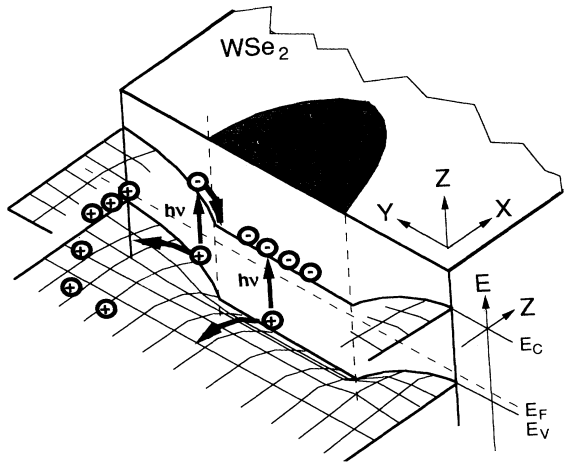


FIG. 15. Schematic model of the energetic conditions of the clustered $p$-$WSe_2$ (0001)/In interface. Band bending and charge-carrier transport is expected normal and parallel to the surface with the origin below the In cluster.

$$d_s = \left[ \frac{\varepsilon \varepsilon_0 V_b}{2\pi e N_A} \right]^{1/2} \tag{1}$$

and taking $V_b = 1$ V, $\varepsilon = 7.3$ (Ref. 47), and $N_A = 10^{17}$ cm$^{-3}$ we obtain a depletion layer width $d_s$ of about 250 Å. Following the calculation of Miyano *et al.*[15] the lateral depletion width is even smaller than this one-dimensional value. Compared to the measured cluster distance distribution as obtained from STM and SEM data the value of $d_s$ should result in a laterally inhomogeneous electric potential distribution (lateral band bending) as shown qualitatively in Fig. 15. It should be noted at this point that lateral inhomogeneous electric potential distributions at clustered metal/semiconductor interfaces have been expected and theoretically discussed for III-V semiconductors.[15] However, the theoretical expectations could not be proven experimentally up to now.[15] For this reason it was considered that on clustered III-V semiconductor/metal interfaces intercluster surface states are formed even on bare areas which result in a pinning situation. The (0001) van der Waals surface of $WSe_2$ is evidently a counterexample, which is related to the specific surface properties of the van der Waals plane exhibiting no dangling bonds or surface states. In view of this model it is expected that a dense metal overlayer prepared at 100-K sample temperature should result in larger band bending as determined from the substrate BE shifts. Indeed $eV_b$ corrected for SPV is at least 0.9 eV and thus close to the Schottky limit (Fig. 12). Consequently, substrate line widths should be increased by lateral inhomogeneities. We do not get clear experimental evidence for this effect. In the RT deposition experiment ($eV_b = 0.5$ eV), there is indeed some broadening of valence-band and core-level features (XPS with limited resolution). In the LT deposition experiment the small nominal coverage of 20 Å leads to large uncovered areas

with very small $eV_b$ shifts ( $<0.2$ eV, see below and Fig. 13) masking the effect.

### C. SPV in dependence on interface morphology

The SPV shifts of In 4*d* and W 4*f* line positions as a function of coverage at 100 K (Fig. 12) agree with previously published results[42] where the synchrotron-induced SPV nearly disappears due to leakage currents when the metal overlayer is completed (20-Å coverage). There are different mechanisms which may be responsible for noninfinite diode shunt resistances: Either a short to the sample holder is produced or internal shorts to defect sites on the van der Waals plane are produced. After warming up the SPV increases because the short circuit is removed by the clustering of the interface. In the transition regime a strong broadening of the In 4*d* line is observed. The emission feature can be fitted with two single In 4*d* lines. We relate those to still "connected" and already isolated clusters. This leads to the splitting in the In 4*d* SPV curve between 210 and 300 K in the right upper part of Fig. 12. Indeed, the higher 240-K SPV value equals the value obtained by recooling (see below). After reaching 300 K only one emission remains. In the lower part of the figure the W 4*f* shifts compared to the position after cleaving in vacuum (flat-band position) are shown. The curve indicated with triangular markers shows the shifts as measured whereas the quadratic marked curve is obtained by subtracting the In 4*d* SPV shifts from the measured band-bending values. The resulting curve shows the actual band bending without SPV. However, this is valid only for the unclustered interface, i.e., only up to 200 K. At $T>200$ K the W 4*f* BE shifts are mostly due to the uncovering of the substrate and not due to SPV shifts. In order to prove this the clustered interface was cooled down again to 100 K by which the W 4*f* lines shift into flat-band direction caused by increasing SPV at reduced temperatures[20,22] (Fig. 13). The effect is relatively small (0.1 V) for the W 4*f* lines. For the clustered interface a strong SPV-induced shift is only expected for the substrate emission lines below the metal clusters (which, however, are beyond the information depth) and for the In overlayer lines. In the bare areas only small SPV shifts are expected due to the smaller band bending and minority carrier flux from these areas to the In-covered areas (Fig. 15). The SPV-induced shift of the In cluster binding energy is significantly larger and can be used for a determination of the subcluster energy diagram as will be shown below.

Simultaneous with the W 4*f* shift towards flat-band condition, the W 4*f* line width decreases by 0.1 eV (Fig. 13). This effect is small because $eV_b$ is already reduced due to the synchrotron-induced SPV at RT ($eV_b<0.2$ eV). The line width at flat-band conditions after cleaving in vacuum (0.34 eV, also indicated in the diagram) is not changed by cooling to 100 K.

### D. Determination of barrier height and photocurrent from temperature-dependent SPV measurements

According to previously published methods[20,38] for estimating the apparent synchrotron-induced SPV, it was possible to fit the temperature-dependent SPV shift of the In cluster emissions.

Neglecting leakage currents, recombination in the space-charge region and tunneling over the barrier the total current $j_{\text{tot}}$ passing the semiconductor/metal barrier in an idealized photovoltaic device is given by

$$j_{\text{tot}}=j_{\text{th}}-j_{\text{ph}}=j_0(e^{-qV_{\text{SPV}}/kT}-1)-j_{\text{ph}} , \tag{2}$$

where $j_{\text{ph}}$ is the photon-induced current, $j_{\text{th}}$ is the thermionic emission current over the barrier, $V_{\text{SPV}}$ is the SPV, and $j_0$ is the reverse saturation current. $j_0$ can be expressed in the thermionic emission model by[3]

$$j_0=A^*T^2e^{-\Phi_b/kT} , \tag{3}$$

where $A^*$ is the effective Richardson constant and $\Phi_b$ is the barrier height. During photoemission measurements we have approximately open circuit conditions, i.e., $j_{\text{tot}}\approx 0$. Therefore solving Eq. (2) with (3) to $V_{\text{SPV}}$ yields the expression for the open circuit photovoltage:

$$V_{\text{SPV}}=\frac{kT}{q}In\left[\frac{j_{\text{ph}}}{j_0}+1\right] . \tag{4}$$

The In SPV curve of the clustered interface shown in Fig. 14 was fitted with Eq. (4). The fitting parameters were the barrier height $\Phi_b$ and the photoinduced current $j_{\text{ph}}$. The Richardson constant was set to $A^*=120$ assuming an effective mass of $m^*=m_0$ according to exciton binding energy measurements from Anneda.[48] The drawn line in Fig. 14 represents the best fit with

$$j_{\text{ph}}=4.1\times 10^{-2}\ \frac{\text{mA}}{\text{cm}^2} ,$$

$$\Phi_b=1.04\ \text{eV} .$$

For the crystals used (doping density of about $10^{17}$ cm$^{-3}$) the energy difference of $E_F$ to the valence-band maximum is about 0.1 eV. Hence the band bending below the indium clusters can be determined to be 0.9 eV which is close to the actual measured value in the 100-K experiments. The remaining discrepancy can be explained by idealization of the junction and by the temperature-dependent band gap, which has not been taken into account.

The obtained photocurrent density of the transformed $WSe_2$/In junction illuminated with 66-eV synchrotron radiation agrees with recently published estimates[38,49] and is considerably larger than $j_{\text{ph}}$ estimated for the monochromatized synchrotron light originally and expected for the He I and Mg $K\alpha$ radiation [$j_{\text{ph}}(\text{He})=9\times 10^{-4}$ mA/cm$^2$; $j_{\text{ph}}(\text{Mg } K\alpha)=6\times 10^{-3}$ mA/cm$^2$].[50] The SPV obtained in the RT experiment (0.6 V at 150 K) also fits nicely to this calculation indicating that $eV_b$ is also about 0.9 eV below the In cluster and considerably larger than the substrate core-level shifts.

## V. SUMMARY AND CONCLUSION

In this paper we have presented experimental results which indicate the presence of an inhomogeneous lateral surface potential distribution on clustered *p*-$WSe_2$ (0001)/In Schottky barriers. The band bending deter-

mined at the clustered interface is considerably smaller than the actual band bending measured at 100 K for the nonclustered interface. This leads to the conclusion that at clustered interfaces besides SPV corrections also inhomogeneity corrections have to be taken into account when determining the band bending. The inhomogeneity shows up in larger metal cluster SPV shifts compared to the substrate shifts. In addition, SPV measurements as a function of temperature allow the determination of the actual band-bending value below the clusters which could be substantiated by comparison to the measurements of the nonclustered interface. These results differ completely to previously published results on III-IV semiconductor/metal cluster interfaces, which may be taken as evidence for a more ideal junction formation valid for the layered semiconductors without dangling bonds.

## ACKNOWLEDGMENTS

We thank J. Lehmann and H. Sehnert for their technical assistance in performing this work and Y. Tomm for providing the substrate crystals. Furthermore, we are grateful to H. Jungblut for performing the SEM and STM measurements. The work presented here was supported by the BMFT (Contract No. 0328926A).

[1]L. J. Brillson, C. F. Brucker, A. D. Katnani, N. G. Stoffel, R. Daniels, and G. Margaritondo, Surf. Sci. **132**, 212 (1983).
[2]*Metal Semiconductor Schottky Barrier Junctions and Their Applications,* edited by B. L. Sharma (Plenum, New York, 1984).
[3]E. H. Rhoderick and R. H. Williams, in *Metal-Semiconductor Contacts,* edited by P. Hammond and R. L. Grimsdale, Monographs in Electrical and Electronic Engineering (Clarendon, Oxford, 1988), Vol. 19.
[4]J. Bardeen, Phys. Rev. **71**, 717 (1947).
[5]W. Mönch, J. Vac. Sci. Technol. B **6**, 1270 (1988).
[6]W. E. Spicer, Z. Lilienthal-Weber, E. Weber, N. Newman, T. Kendelewicz, R. Cao, C. McCants, R. Mahowald, K. Miyano, and I. Lindau, J. Vac. Sci. Technol. B **6**, 1245 (1988).
[7]J. H. Werner and H. H. Güttler, J. Appl. Phys. **69**, 1522 (1991).
[8]R. T. Tung, Phys. Rev. B **45**, 13 509 (1992).
[9]J. Y. F. Tang and L. Freeouf, J. Vac. Sci. Technol. B **2**, 459 (1984).
[10]K. E. Miyano, R. Cao, T. Kendelewicz, C. J. Spindt, P. H. Mahowald, I. Lindau, and W. E. Spicer, J. Vac. Sci. Technol. B **6**, 1403 (1988).
[11]T. T. Chiang, C. J. Spindt, W. E. Spicer, I. Lindau, and R. Browning, J. Vac. Sci. Technol. B **6**, 1409 (1988).
[12]G. D. Waddill, I. M. Vitomirov, C. M. Aldao, S. G. Anderson, C. Capasso, J. H. Weaver, and Z. Liliental-Weber, Phys. Rev. B **41**, 5293 (1990).
[13]Z. M. Lü, D. Mao, L. Soonckindt, and A. Kahn, J. Vac. Sci. Technol. A **8**, 1988 (1990).
[14]I. M. Vitomirov, C. M. Aldao, G. D. Waddill, C. Capasso, and J. H. Weaver, Phys. Rev. B **41**, 8465 (1990).
[15]K. E. Miyano, D. M. King, C. J. Spindt, T. Kendelewicz, R. Cao, Z. Yu, I. Lindau, and W. E. Spicer, Phys. Rev. B **43**, 11 806 (1991).
[16]S. P. Svensson, J. Kanski, and T. G. Andersson, Phys. Rev. B **30**, 6033 (1984).
[17]D. E. Savage and M. G. Lagally, J. Vac. Sci. Technol. B **4**, 943 (1986).
[18]Z. Liliental-Weber, E. R. Weber, J. Washburn, and J. H. Weaver, Appl. Phys. Lett. **56**, 2507 (1990).
[19]J. B. Adams, W. N. G. Hitchon, and L. M. Holzmann, J. Vac. Sci. Technol. A **6**, 2029 (1988).
[20]M. H. Hecht, Phys. Rev. B **41**, 7918 (1990).
[21]M. H. Hecht, J. Vac. Sci. Technol. B **8**, 1018 (1990).
[22]K. Horn, M. Alonso, and R. Cimino, Appl. Surf. Sci. **56-58**, 271 (1992).
[23]W. Jaegermann, in *Photoelectrochemistry and Photovoltaics of Layered Semiconductors,* edited by A. Aruchamy (Kluwer Academic, Dordrecht, 1992), p. 195.
[24]R. H. Williams, A. McKinley, G. J. Hughes, V. Montgomery, and I. T. McGovern, J. Vac. Sci. Technol. **21**, 594 (1982).
[25]W. Jaegermann, C. Pettenkofer, and B. A. Parkinson, Phys. Rev. B **42**, 7487 (1990).
[26]D. W. Pashley, M. J. Stowell, M. H. Jacobs, and T. J. Law, Philos. Mag. **10**, 127 (1964).
[27]M. H. Jacobs, D. W. Pashley, and M. J. Stowell, Philos. Mag. **13**, 129 (1966).
[28]M. Kamaratos and C. Papageorgopoulos, Solid State Commun. **49**, 715 (1984).
[29]S. Kennou, S. Ladas, and C. Papageorgopoulus, Surf. Sci. **152/153**, 1213 (1985).
[30]S. Ladas, S. Kennou, M. Kamaratos, S. D. Foulias, and C. Papageorgopoulos, Surf. Sci. **189/190**, 261 (1987).
[31]M. L. Bortz, F. S. Ohuchi, and B. A. Parkinson, Surf. Sci. **223**, 285 (1989).
[32]T. Ichinokawa, T. Ichinose, M. Tohyama, and H. Itoh, J. Vac. Sci. Technol. A **8**, 500 (1990).
[33]I. T. McGovern, E. Dietz, H. H. Rotermund, A. M. Bradshaw, W. Braun, W. Radlik, and J. F. McGilp, Surf. Sci. **152/153**, 1203 (1985).
[34]I. T. McGovern, J. F. McGilp, G. J. Hughes, A. McKinley, R. H. Williams, and D. Norman, Vacuum **33**, 607 (1983).
[35]J. R. Lince, D. J. Carré, and P. D. Fleischauer, Phys. Rev. B **36**, 1647 (1987).
[36]R. Schlaf, H. Sehnert, C. Pettenkofer, and W. Jaegermann, in *Heteroepitaxy of Dissimilar Materials,* edited by R. F. C. Farrow, J. P. Harbison, P. S. Peercy, and A. Zangwill, MRS Symposia Proceedings No. 221 (Materials Research Society, Pittsburgh, 1991), p. 137.
[37]I. Kojima and M. Kurahashi, J. Electron. Spectrosc. Relat. Phenom. **42**, 177 (1987).
[38]A. Schellenberger, R. Schlaf, C. Pettenkofer, and W. Jaegermann, Phys. Rev. B **45**, 3538 (1992).
[39]C. Argile and G. E. Rhead, Surf. Sci. Rep. **10**, 277 (1989).
[40]A. Klein, C. Pettenkofer, and W. Jaegermann (unpublished).
[41]D. A. Evans, M. Alonso, R. Cimino, and K. Horn, Phys. Rev. Lett. **70**, 3483 (1993).
[42]G. D. Waddill, T. Komeda, Y.-N. Yang, and J. H. Weaver, Phys. Rev. B **41**, 10 283 (1990).
[43]D. E. Savage and M. G. Lagally, Phys. Rev. Lett. **55**, 959 (1985).
[44]C. J. Spindt, R. Cao, K. E. Miyano, I. Lindau, W. E. Spicer, and Y.-C. Pao, J. Vac. Sci. Technol. B **8**, 974 (1990).
[45]R. Cimino, A. Giarante, M. Alonso, and K. Horn, Appl. Surf. Sci. **56-58**, 151 (1992).
[46]J. Peisner, P. Roboz, and P. B. Barna, Phys. Status Solidi A **4**,

K187 (1971).

[47]The dielectric constants of the layered materials are strongly anisotropic. The two values are $\varepsilon = 12.7$ (perpendicular to the $c$ axis) and $\varepsilon = 4.2$ (parallel to the $c$ axis); A. R. Beal and W. Y. Liang, J. Phys. C **9**, 2449 (1976); **9**, 2459 (1976).

[48]A. Anedda, E. Fortin, and F. Raga, Can. J. Phys. **57**, 368 (1979).

[49]S. Chang, I. M. Vitomirov, L. J. Brillson, D. F. Rioux, P. D. Kirchner, G. D. Pettit, J. M. Woodall, and M. H. Hecht, Phys. Rev. B **41**, 12 299 (1990).

[50]The photocurrent densities are calculated using photon intensities of $10^{12}$ cm$^{-2}$ s$^{-1}$ for He I and of $10^{11}$ cm$^{-2}$ s$^{-1}$ for Mg $K\alpha$. A quantum efficiency of 1 is assumed.

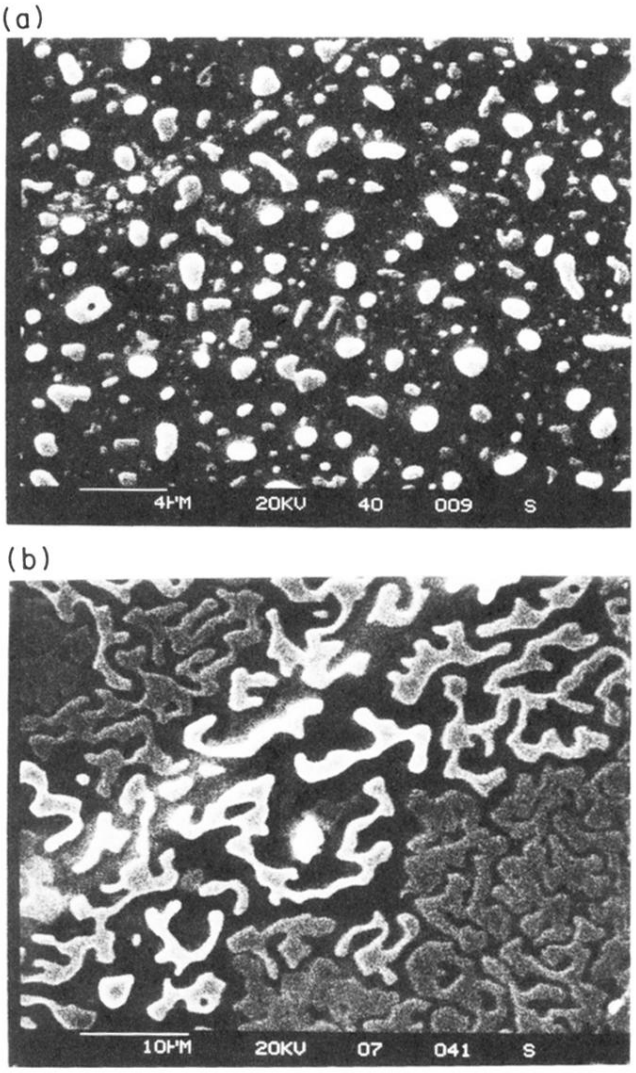


FIG. 4. Scanning-electron-microscope pictures of the $WSe_2$/In interface for different nominal coverages [(a) 80 Å, (b) 560 Å].

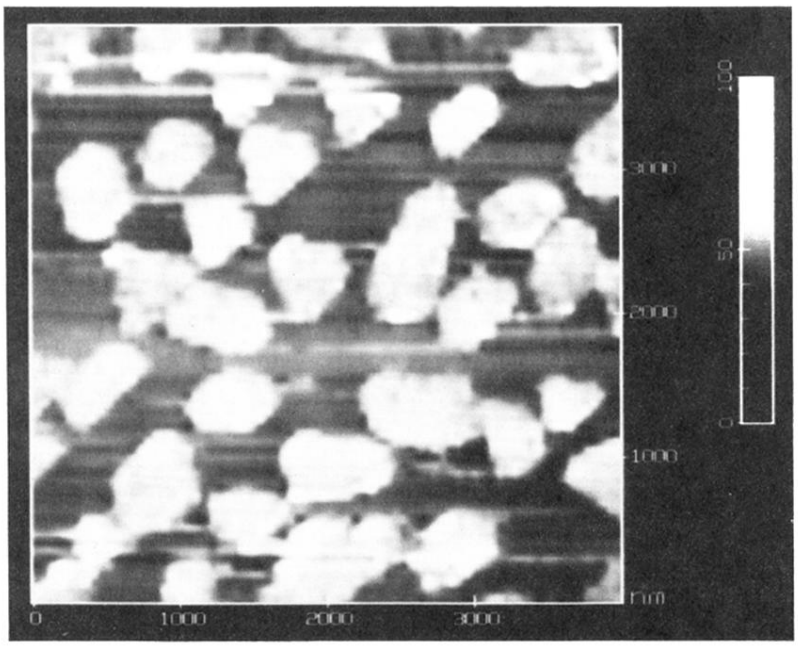


FIG. 5. Scanning-tunneling-microscope picture of the $WSe_2$/In interface at a nominal coverage of 40 Å.